Scientific Foundation SPIROSKI, Skopje, Republic of Macedonia
Open Access Macedonian Journal of Medical Sciences. 2022 Jul 15; 10(A):1278-1284.
https://doi.org/10.3889/oamjms.2022.10005
eISSN: 1857-9655
**Category:** *A - Basic Sciences*
***Section:*** *Pharmacology*





# Primaquine-chitosan Nanoparticle Improves Drug Delivery to Liver Tissue in Rats

Melva Louisa[1]*, Putrya Hawa[2], Purwantyastuti[1], Etik Mardliyati[3], Hans-Joachim Freisleben[4,5]

*[1]Department of Pharmacology and Therapeutics, Faculty of Medicine, Universitas Indonesia, Jakarta, Indonesia; [2]Master Program in Biomedical Sciences, Faculty of Medicine, Universitas Indonesia, Jakarta, Indonesia; [3]Center for Pharmaceutical and Medical Technology, Agency for the Assessment and Application of Technology, Serpong, Indonesia; [4]German-Indonesian Medical Association (DIGM), Bad Mergentheim, Germany; [5]Medical Research Unit, Faculty of Medicine, Universitas Indonesia, Jakarta, Indonesia*

**Edited by:** Sinisa Stojanoski
**Citation:** Louisa M, Hawa P, Purwantyastuti, Mardliyati E, Freisleben H. Primaquine-chitosan Nanoparticle Improves Drug Delivery to Liver Tissue in Rats. Open-Access Maced J Med Sci. 2022 Jul 15; 10(A):1278-1284. https://doi.org/10.3889/oamjms.2022.10005
**Keywords:** 8-Aminoquinoline; Antimalarial; Hypnozoite; Nanoformulation; *Plasmodium vivax*; Pharmacokinetics
***Correspondence:** Melva Louisa, Department of Pharmacology and Therapeutics, Faculty of Medicine, Universitas Indonesia; Jl. Salemba Raya No. 6, Jakarta Pusat, Jakarta, Indonesia. E-mail: melva.louisa@gmail.com
**Received:** 29-Apr-2022
**Revised:** 30-Jun-2022
**Accepted:** 05-Jul-2022

**Funding:** This study was supported by Universitas Indonesia
**Competing Interest:** The authors have declared that no competing interest exists


**Abstract**

**BACKGROUND:** Primaquine is one of the essential medicines used to treat malaria due to Plasmodium vivax. Primaquine works by destroying hypnozoites in the liver, and its effectiveness is based on the concentration of the drug in the target tissue. Primaquine acts by eradicating hypnozoites in the liver, and its effect is dependent on the drug concentrations in the target tissue.

**AIM:** The present study aimed to prepare primaquine in nanoparticle formulation using chitosan as carriers and improve on-target primaquine delivery to the liver.

**METHODS:** Primaquine-loaded chitosan nanoparticles were prepared using the ionic gelation method variations. Then, the resulting primaquine-chitosan nanoparticles were administered to the rats and compared with conventional primaquine. Afterward, plasma and liver concentrations of primaquine were quantified.

**RESULTS:** The primaquine-chitosan nanoparticles obtained were at 47.9 nm. The area under the curve (AUC) for primaquine-chitosan nanoparticles resulted lower in the AUC and Cmax, 0.46 and 0.42 times of conventional primaquine, respectively. However, no differences were found in time to reach Cmax (Tmax). Primaquine liver concentrations obtained with primaquine-chitosan primaquine nanoparticles resulted in 3 times higher than primaquine concentration.

**CONCLUSION:** Enhanced drug delivery to rat liver tissue by primaquine-chitosan nanoparticles may improve on-target drug delivery to the liver, enhance primaquine ant hypnozoites effects, and reduce unwanted side effects in the circulation.

## Introduction

Malaria due to *Plasmodium vivax* is a severe hazard to human health across the globe, being the most widely distributed species of the five plasmodia known to infect humans [1], [2]. Unlike malaria due to *Plasmodium falciparum*, patients infected with *Plasmodium vivax* and *Plasmodium ovale* often experience recurrent infections. In addition, hypnozoites, latent liver stage parasites, are the source of relapse in malaria [1], [3].

Activation of hypnozoites, the liver-stage parasites that lie latent after initial infection, is how *P. vivax* may induce relapses weeks or months after the first infection. The hypnozoite reservoir of the disease consists of these latent liver-stage infections. It is possible for these persistent phases of infection to reactivate and reproduce for months, even years, after the primary clinical illness, causing relapse and recurrence of transmission. The hypnozoite reservoir, which is undetected and unaffected by most antimalarial medications, is a significant barrier to the treatment and eradication of malaria [4], [5].

A radical cure of vivax malaria can only be achieved using the 8-aminoquinolines, including primaquine and tafenoquine. Relapses after vivax malaria infections can be prevented by the hypnozoitocidal effects of primaquine and tafenoquine [3]. Primaquine is generally tolerable and safe. Primaquine has certain drawbacks, such as a lack of lipophilicity that may restrict its liver absorption and a rapid metabolism that results in an inactive metabolite [6], [7]. Drug modification to nano-sized therapeutic formulations may be able to tackle many of the challenges of enhancing absorption, on-target bioavailability, and drug accumulation [8].

Thus, in the present study, we aimed to prepare primaquine nanoparticles utilizing chitosan as a carrier to enhance drug transport to the liver and investigate the pharmacokinetic profile of primaquine nanoparticles administered orally in the rats.

## Materials and Methods

### *Materials*

Chitosan (degree of deacetylation ± 85%), natrium tripolyphosphate, and primaquine were purchased from Sigma-Aldrich (USA). Phosphate buffer, acetonitrile, methanol, diethyl ether, NaOH, Tris-buffer, trichloroacetic acid (TCA), sodium azide, bovine serum albumin, and acetic acid glacial were purchased from Merck (Darmstadt, Germany). All other reagents used were of analytical grade.

The high-performance liquid chromatography (HPLC) device used include: Waters™ Intelligent Sample Processor 2695 equipped with Degasser separation; Inertsil™ ODS-4 column (4.6 × 150 mm, 5 μm), and Waters™ Photodiode Array Detector (PDA) 2998.

### *Primaquine nanoparticle preparation*

The formation of nanoparticles resulted from the interaction between negatively charged phosphate groups from TPP and the positively charged amino groups of chitosan [9]. Nano-sized primaquine was obtained upon the dropwise addition of aqueous tripolyphosphate (TPP) solution to chitosan solutions followed by continuous stirring at 300–400 rpm at room temperature. Before adding TPP/chitosan, primaquine was dissolved in the chitosan or TPP solution.

### *Particle size distribution analysis, polydispersity index, and zeta potential*

Particle size distribution and zeta potential were determined by a Malvern Particle Sizer (Malvern® Instruments, UK) or a Delsa® Nanosizer/Zeta Potential Analyzer (Beckmann-Coulter) at Nanotech Indonesia, PUSPIPTEK Serpong.

### *Morphology analysis of primaquine nanoparticles*

We determined the morphology of primaquine nanoparticles using the Transmission Electron Microscope (TEM) in the Faculty of Chemistry, Gadjah Mada University, Yogyakarta.

### *The entrapment efficiency of primaquine nanoparticles*

The amount of primaquine in the nanoparticles was measured using UV spectrophotometry. Preliminary studies obtained the absorbance maximum of primaquine at wavelength λ 259.3 nm. Nanoparticle samples were centrifugated at 12,000 rpm for 15 min. We calculated the difference between the total amount of primaquine used for the preparation of primaquine nanoparticles and the amount of free primaquine in the supernatant to assess the entrapment efficiency of nanoparticles [10].

$$EE = \frac{[(\text{Total amount of drug}) - (\text{The amount of free drug})]}{(\text{Total amount of drug})} \times 100\%$$

### *Evaluation of primaquine concentrations in plasma, liver, and pharmacokinetic profiles of primaquine nanoparticles versus conventional primaquine*

Twelve Sprague Dawley rats were used in the parallel-controlled pharmacokinetic investigation. Our experiment was approved by the Faculty of Medicine Universitas Indonesia's Ethics Committee before it began. The animals were kept in the animal house with unlimited access to a standard diet and drinking water. The 12 rats were randomly divided into two treatment groups of six to receive conventional primaquine group 15.5 mg/kg BW orally or primaquine nanoparticle 15.5 mg/kg BW. Treatment was given once daily for 5 days. Primaquine dose selected was based on the equivalence to human dose and calculated based on dose translation using body surface area [11], [12], [13].

On the 5$^{th}$ day of the experiment, blood was collected from the tail vein before to the last drug administration, then 30, 60, 90, 120, 180, and 240 min later. Subsequently, rats were decapitated, and the livers excised.

### *Analysis of primaquine in plasma and liver*

Drug concentrations in rat and liver plasma were done using high-performance liquid chromatography (HPLC). A researcher in our laboratory previously validated the HPLC methods used [14]. For the present study, we did a partial validation test to ensure the usability of the applied method [15]. HPLC column used was connected to a column heater and set at 40°C. The Waters Photodiode Array Detector (PDA) 2998 was adjusted to a wavelength of λ 255 nm. The HPLC device was completed by Hewlett-Packard Reporting Integrator #3392A (Hewlett-Packard Co., Santa Clara, CA). The mobile HPLC phase consisted of a phosphate buffer (20 mM, pH 3.0), acetonitrile, and methanol 70% with a volume ratio of 65:15:20. The materials for evaluating drug concentrations were phosphate buffer pH 3.0, methanol 70%, diethyl ether, NaOH 0.1 N, Tris-buffer, trichloroacetic acid (TCA) 10%, acetonitrile, sodium azide, bovine serum albumin (BSA), and distilled water.

Blood samples were centrifuged at 3000 rpm for 5 min to obtain the rat plasma. Sample extraction of

primaquine from plasma was initiated by adding 50 μL of NaOH 0.1 to the sample. Afterward, 1 mL of diethyl ether was mixed into the sample solution followed by centrifugation. Then, the supernatant was pipetted and dried under nitrogen. Subsequently, the samples were diluted in phosphate buffer and inserted into the HPLC.

Ultra-Turrax was used to homogenize the liver sample for analysis. A 1:1 volume ratio of Tris-buffer was added to liver homogenates. Afterward, the homogenates were centrifugated at 3000 rpm for 10 min to collect the supernatant. Trichloroacetic acid solution at a ratio of 1:1.5 to the supernatant was added to denature the remaining protein in the solution. Subsequently, the samples were recentrifuged at 8000 rpm for 2 min to precipitate protein and collect the supernatant. Afterward, sample extraction steps, from the addition of NaOH to the dilution of phosphate buffer, were done as that of plasma.

### *Data analysis*

We used drug concentration in plasma which was to calculate the pharmacokinetic parameters of primaquine nanoparticles and conventional primaquine. The area under the curve (AUC) was calculated using the trapezoidal method. Absorption rate constant ($k_a$), elimination rate constant ($k_e$), absorption phase half-life ($t_{1/2\ abs}$), and elimination phase half-life ($t_{1/2\ el}$) were calculated from regression of equation ln Ct to T [16]. A comparison of plasma and liver concentrations between primaquine nanoparticles, and conventional primaquine was carried out by independent t-test in GraphPad Prism version 9.3.1.

## Results

### *Optimum primaquine-chitosan nanoparticle formulation*

Chitosan nanoparticles are made through ionic gelation between positively charged chitosan and negatively charged tripolyphosphate [17]. Following 18 variations of nanoparticle preparation, the final formula used for further evaluation was formula 19: 0.1% chitosan solution in 0.15% acetic acid, 0.5% Na-TPP solution, and 0.3% primaquine diphosphate. The method used to obtain optimum nano-size primaquine was by slow infusion of the mixture followed by stirring at 400 rpm for 15 min.

### *Particle size distribution and morphological shape of nano-primaquine-chitosan*

Out of the 20 preparation variations, primaquine particle size distributions ranged from 50 to 250 nm, with entrapment efficiency of up to 55%. The final formula used for further experiments, including *in vivo* study, resulted in a particle size distribution of 47.9 ± 13.7 nm (Figure 1), polydispersity index (P.I.) 0.313, and cumulative number distribution of 100%, that is, the peak contained all particles measured.

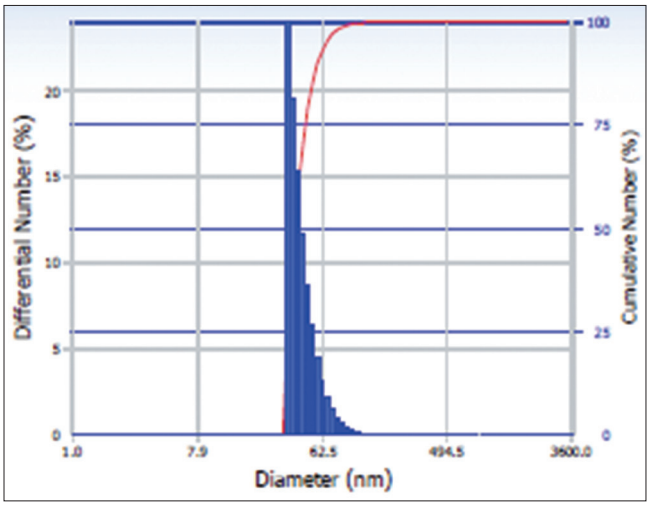


*Figure 1: Particle size distribution of the primaquine-chitosan nanoparticle final formulation. The particle size distribution obtained was at 47.9 ± 13.7 nm, polydispersity index (P.I.) 0.313. The cumulative number of 100%, which showed that there is only one peak that contained all particles from this preparation*

Morphological examination of primaquine-chitosan nanoparticles by transmission electron microscopy (TEM) showed a spherical shape (Figure 2).

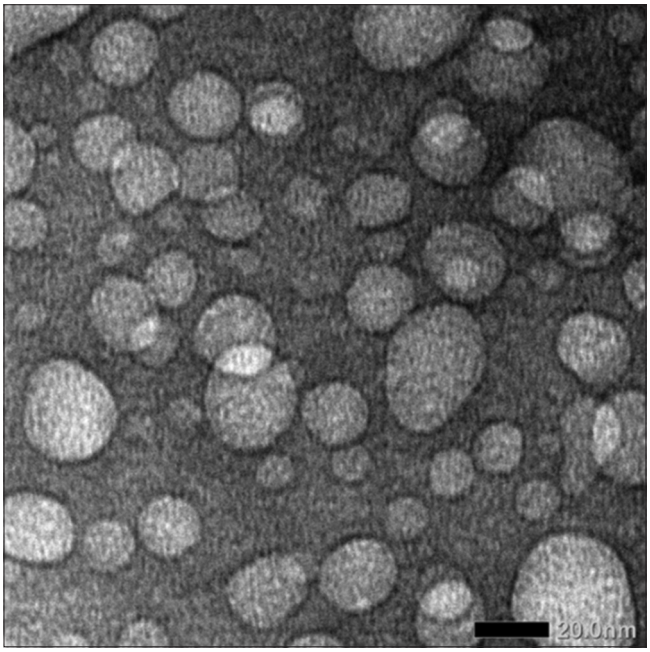


*Figure 2: Transmission electron micrograph of primaquine-chitosan nanoparticles. The bar shown equals 20 nm*

### *Zeta potential of nano-primaquine-chitosan*

Zeta potential greatly influences particle stability in suspension through the electrostatic repulsion between particles. It also determines the interaction of nanoparticles

with cell membranes, which are usually negatively charged [17]. Figure 3 displays the zeta potential of primaquine nanoparticles with a peak at + 18.52 mV.

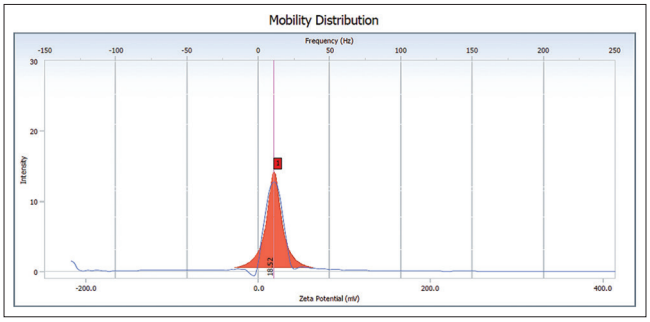


*Figure 3: Zeta potential of primaquine-chitosan nanoparticle preparation (at +18.52 mV)*

### *Entrapment efficiency of nano-primaquine-chitosan*

Entrapment efficiency (EE) of nanoparticle formulation was at 54.7% of primaquine.

### *Partial validation of primaquine quantification method*

We did a partial validation of the previously developed and validated methods to ensure the applicability of the quantification of our sample [14], [15]. All our results meet the criteria for partial validation [15]. Accuracy of primaquine was ranged from 1.37 to 6.37% in low concentrations, 0.16–1.1% in medium concentrations, and 0.17–1.03% in high concentrations. Primaquine concentrations in samples showed that precision tests ranged from 6 to 10%. Linearity tests of primaquine standards meet linear regression values with R ranging from 0.9994 to 0.9998. Primaquine in both plasma and liver samples had a limit of detection (LOD) and limit of quantification (LOQ) of 0.05 μL/mL and 0.15 μL/mL, respectively. The recovery percentage in conventional primaquine samples ranged from 90 to 107%.

### *Primaquine and nano-primaquine concentrations in plasma and liver*

Primaquine and nano-primaquine concentrations in plasma at each interval of blood collection time after drug administration are listed in Table 1.

On the 5$^{th}$ day, the liver was harvested at 4 h following the dose of primaquine. Nano-primaquine concentrations in the liver were significantly higher (3 times; $p < 0.05$) than conventional primaquine (Table 2).

### *Pharmacokinetic profile of primaquine and nano-primaquine*

The AUC of primaquine nanoparticles was significantly lower (3.3 times; $p < 0.05$) than of conventional primaquine. In addition, the maximum concentration in plasma ($C_{max}$) of nano-primaquine was 2.3 times smaller than that of conventional primaquine. After 90 min of medication administration, the highest levels of primaquine and nano-primaquine were attained (Table 3).

**Table 1: Primaquine concentrations in rat plasma after drug administration of conventional primaquine or nano-primaquine-chitosan**

| Samples drawn at min' | Primaquine (μg/mL) | Primaquine nanoparticles (μg/mL) | 95% confidential interval | p value ($p < 0.05$) |
|---|---|---|---|---|
| 0' | 0.01 ± 0.00 | 0.19 ± 0.00 | | |
| 30' | 0.97 ± 0.01 | 0.44 ± 0.02 | 0.434; 0.626 | 0.0018* |
| 60' | 1.26 ± 0.15 | 0.57 ± 0.02 | −0.423; 5.624 | 0.6057 |
| 90' | 1.77 ± 0.11 | 0.75 ± 0.02 | 0.539; 1.501 | 0.0118* |
| 120' | 1.24 ± 0.12 | 0.51 ± 0.01 | 0.228; 1.222 | 0.0244* |
| 180' | 0.47 ± 0.01 | 0.37 ± 0.02 | 0.006; 0.184 | 0.0440* |
| 240' | 0.23 ± 0.02 | 0.29 ± 0.00 | −0.130; 0.005 | 0.0493* |

*Significant at $P < 0.05$.

**Table 2: Primaquine concentrations in rat liver after drug administration of conventional primaquine or nano-primaquine-chitosan**

| Samples | Primaquine (μg/mL) | Primaquine nanoparticles (μg/mL) | 95% confidential interval | p-value |
|---|---|---|---|---|
| 240 min | 0.48 ± 0.04 | 1.45 ± 0.01 | -1.138; 0.791 | 0.0017* |

*Significant at $P < 0.05$.

## Discussion

In the present study, we displayed that chitosan as a carrier is an effective method to obtain nano-sized primaquine with drug absorption and distribution to the liver.

Chitosan is a natural polymer generated by partial deacetylation of chitin. After cellulose, chitin is the most common polysaccharide in the natural world. It is non-toxic, biocompatible, and biodegradable. As a pharmacological carrier, chitosan has been widely used by researchers in various drug applications to produce a targeted drug delivery system [9], [18], [19], [20], [21]. In addition, a study by Wimardani *et al*. has shown that chitosan at high concentrations might have cytotoxic effects on oral cancer cell lines [22]. In the present study, we only use a low concentration of chitosan (0.3%) as a carrier for primaquine.

Primaquine is a hydrophobic compound *per se* and becomes water soluble through its reaction to diphosphate salt. The primaquine diphosphate mimics the tripolyphosphate interaction with chitosan, which may be a reason for the relatively easy and effective incorporation of about 55% of the compound into the nanoparticles. Recently, a working group in India published primaquine nanoparticles with an even higher entrapment of more than 90% of primaquine [23]. Hence, the scope of our future work will be to enhance our entrapment rates.

Out of 20 preparation variations, the best formulation resulted in a single peak particle distribution at 47.9 nm, which can be therapeutically valuable due

**Table 3: Pharmacokinetic profile of conventional primaquine and primaquine-chitosan nanoparticles**

| Pharmacokinetic parameters | Primaquine | Primaquine-chitosan nanoparticles | 95% confidence interval | p-value |
|---|---|---|---|---|
| AUC (μg/mL) | 3.54 ± 0.023 | 1.66 ± 0.155 | 1.76; 2.01 | <0.001* |
| Cmax ((μg/mL) | 1.77 ± 0.11 | 0.75 ± 0.02 | 0.5389; 1.5011 | 0.0118* |
| Tmax (h) | 1.5 | 1.5 | - | - |
| Ka (per h) | 1.53 ± 0.11 | 1.96 ± 0.32 | 1.88; 1.03 | 0.336 |
| Ke (per h) | 0.85 ± 0.01 | 0.28 ± 0.01 | 0.47; 0.63 | <0.001* |
| $t_{1/2abs}$ (h) | 0.45 ± 0.03 | 0.36 ± 0.06 | −0.20; 0.38 | 0.313 |
| $t_{1/2el}$ (h) | 0.82 ± 0.01 | 2.46 ± 0.08 | −2.02; −1.27 | 0.0027* |
| Clearance (L/h) | 0.87 ± 0.01 | 1.88 ± 0.18 | −1.76; −0.25 | 0.0291* |
| Vd (L) | 1.03 ± 0.02 | 6.65 ± 0.39 | −7.30; −3.94 | 0.0048* |

AUC: Area under the curve, $C_{max}$: Maximum concentration, $T_{max}$: Time to reach $C_{max}$, $k_a$: Absorption rate constant, $t_{1/2\ absorption}$: Absorption phase half-life, $k_e$: Elimination rate constant, $t_{1/2\ elimination}$: Elimination phase half-life, $V_d$: The volume of distribution. *Significant at P < 0.05.

to the method of administration and the target organ or tissue. Furthermore, the result of transmission electron microscopy showed homogenous particles with spherical shapes, which confirmed our findings.

Our findings on the particle size were confirmed with the morphological examination using transmission electron microscopy. The shape supports the particle size equivalent to or close to their diameter. The form of the line describes an almost ideal Gaussian distribution with a peak volume of 45%, which means that the particle population of 47.9 ± 13.7 nm comprises 45% of the total particle volume of the preparation.

Our formulation also achieved an excellent cumulative distribution number of 100%. Furthermore, the distribution number showed that the preparation has only one population peak, that is, uniform distribution with a calculated polydispersity index (P.I.) of 0.313.

The Beckman-Coulter Nanosizer +18.5 mV measured zeta potential in our final formulation, which impacts the stability of the dispersion. Values around 20 mV are considered sufficient for the repulsion between uniformly charged particles to keep them dispersed [24]. However, we have not yet determined the shelf stability of our particles. Our study has only measured the primaquine concentrations in the formulation for up to 1 week, which is currently enough for our *in vivo* study design. Shelf stability of at least 3–6 months would be desirable [25], [26]. Increasing zeta potential (if necessary) might be another aim of future studies, which can be achieved by varying the degree of deacetylation. It is, nevertheless, important to note that the zeta potential (mainly the pH of the outer phase) substantially influences the stability of the nanoparticle dispersion during storage [24].

Our pharmacokinetic study results demonstrated that we had reached the aim to increase the drug delivery to the liver. The concentration in the blood (measured as plasma levels) was lower and in liver tissue 3 times higher than with conventional primaquine, indicating a much stronger distribution into the liver. On the other hand, the elimination rate was also lower with primaquine nanoparticles indicating a depot effect in the liver, an additional pharmacokinetic effect supporting our therapeutic intention.

Our results show that nanoparticles enhance drug delivery to the liver. A higher concentration of nanoparticles in the liver was due to their nano-size structure increasing the surface area, which leads to increased permeation and absorption through cell membranes [17], [23]. Besides, polycationic chitosan nanoparticles with higher surface charge density may interact more intensively with the cell membrane and lengthen the absorption period [17], [27].

The lower AUC of primaquine-chitosan nanoparticles will reduce the dose-limiting side effects of primaquine in plasma, such as hemolytic anemia in patients with G6PD deficiency or methemoglobinemia, and other adverse effects related with higher primaquine plasma concentrations [28], [29].

The absorption rate constant and absorption phase half-life of nanoparticles were statistically not different from primaquine. The finding suggests that nanoparticles did not influence drug absorption in the gastrointestinal tract. The elimination rate constant and elimination phase half-life of nanoparticles exceeded 3 times the values of conventional primaquine, indicating a “depot effect” of nanoparticles in the liver, which decreases free drug concentration in plasma and thus decreases drug elimination from plasma [16], [30].

The organ distribution volume of nano-primaquine was 6.5 times higher than that of conventional primaquine. After 240 min, primaquine nanoparticles reached a roughly threefold higher concentration in the liver than conventional primaquine. Primaquine nanoparticles were highly distributed at the site of pharmacological action. On the other hand, the more than 2-fold lower AUC and concentration of primaquine nanoparticles in plasma will certainly reduce unwanted adverse effects related to high plasma concentrations. Hence, we can conclude that chitosan nanoencapsulation widens the therapeutic window of primaquine by a factor of more than 6, matching the 6.5 times increased volume of distribution in favor of its target organ [16], [31].

## Conclusion

Primaquine nanoparticles obtained using chitosan as a carrier had an ideal particle size distribution and good entrapment efficiency. Furthermore, *in vivo* study in the rats showed that nanoencapsulation successfully enhanced primaquine delivery to the liver. Future studies should optimize our nanoparticle preparation’s entrapment efficacy, stability, and reproducibility and

explore the potential clinical application of primaquine-chitosan nanoparticles in antimalarial therapy.

## References


1. Baird JK. Basic research of *Plasmodium vivax* biology enabling its management as a clinical and public health problem. Front Cell Infect Microbiol. 2021;11:696598.
2. Battle KE, Lucas TC, Nguyen M, Howes RE, Nandi AK, Twohig KA, *et al*. Mapping the global endemicity and clinical burden of *Plasmodium vivax*, 2000-17: A spatial and temporal modelling study. Lancet. 2019;394(10195):332-43. https://doi.org/10.1016/S0140-6736(19)31096-7
   PMid:31229233
3. White NJ. Anti-malarial drug effects on parasite dynamics in vivax malaria. Malar J. 2021;20(1):161. https://doi.org/10.1186/s12936-021-03700-7
   PMid:33743731
4. Howes RE, Battle KE, Mendis KN, Smith DL, Cibulskis RE, Baird JK, *et al*. Global Epidemiology of *Plasmodium vivax*. Am Soc Trop Med Hyg. 2016;95 6 Suppl:15-34. https://doi.org/10.4269/ajtmh.16-0141
   PMid:27402513
5. Schäfer C, Zanghi G, Vaughan AM, Kappe SH. *Plasmodium vivax* latent liver stage infection and relapse: Biological insights and new experimental tools. Annu Rev Microbiol. 2021;75:87-106. https://doi.org/10.1146/annurev-micro-032421-061155
   PMid:34196569
6. Wu C, Qu G, Wang L, Cao S, Xia D, Wang B, *et al*. Clinical characteristics and inflammatory immune responses in COVID-19 patients with hypertension: A retrospective study. Front Pharmacol. 2021;12:721769. https://doi.org/10.3389/fphar.2021.721769
   PMid:34759820
7. Zorc B, Perković I, Pavić K, Rajić Z, Beus M. Primaquine derivatives: Modifications of the terminal amino group. Eur J Med Chem. 2019;182:111640. https://doi.org/10.1016/j.ejmech.2019.111640
   PMid:31472472
8. Kirtane AR, Verma M, Karandikar P, Furin J, Langer R, Traverso G. Nanotechnology approaches for global infectious diseases. Nat Nanotechnol. 2021;16(4):369-84. https://doi.org/10.1038/s41565-021-00866-8
   PMid:33753915
9. Dustgani A, Farahani EV, Imani M. Preparation of chitosan nanoparticles loaded by dexamethasone sodium phosphate. Iran J Pharm Sci. 2008;4:111-4.
10. Cho Y, Shi R, Ben Borgens R. Chitosan nanoparticle-based neuronal membrane sealing and neuroprotection following acrolein-induced cell injury. J Biol Eng. 2010;4(1):2. https://doi.org/10.1186/1754-1611-4-2
    PMid:20205817
11. Popovici J, Tebben K, Witkowski B, Serre D. Primaquine for *Plasmodium vivax* radical cure: What we do not know and why it matters. Int J Parasitol Drugs Drug Resist. 2021;15:36-42. https://doi.org/10.1016/j.ijpddr.2020.12.004
    PMid:33529838
12. Blanchard OL, Smoliga JM. Translating dosages from animal models to human clinical trials-revisiting body surface area scaling. FASEB J. 2015;29(5):1629-34. https://doi.org/10.1096/fj.14-269043
    PMid:25657112
13. Nair A, Morsy MA, Jacob S. Dose translation between laboratory animals and human in preclinical and clinical phases of drug development. Drug Dev Res. 2018;79(8):373-82. https://doi.org/10.1002/ddr.21461
    PMid:30343496
14. Juliati J. Effect of Piperaquine on Pharmacokinetics of Primaquine in Combincation in Primaquine and Piperaquine in Rats. Indonesia: Universitas Indonesia; 2012.
15. Briggs RJ, Nicholson R, Vazvaei F, Busch J, Mabuchi M, Mahesh KS, *et al*. Method transfer, partial validation, and cross validation: Recommendations for best practices and harmonization from the global bioanalysis consortium harmonization team. AAPS J. 2014;16(6):1143-8. https://doi.org/10.1208/s12248-014-9650-3
    PMid:25190270
16. Bauer LA. Clinical pharmacokinetic equations and calculations. In: Bauer LA, editor. Applied Clinical Pharmacokinetics, 2nd ed., Ch. 2. New York, NY: The McGraw-Hill Companies; 2008.
17. Qi L, Xu Z, Jiang X, Hu C, Zou X. Preparation and antibacterial activity of chitosan nanoparticles. Carbohydr Res. 2004;339(16):2693-700. https://doi.org/10.1016/j.carres.2004.09.007
    PMid:15519328
18. Mohammed MA, Syeda JT, Wasan KM, Wasan EK. An overview of chitosan nanoparticles and its application in non-parenteral drug delivery. Pharmaceutics. 2017;9(4):53. https://doi.org/10.3390/pharmaceutics9040053
    PMid:29156634
19. Katas H, Raja MAG, Lam KL. Development of chitosan nanoparticles as a stable drug delivery system for protein/siRNA. Int J Biomater. 2013;2013:146320. https://doi.org/10.1155/2013/146320
    PMid:24194759
20. Herdiana Y, Wathoni N, Shamsuddin S, Muchtaridi M. Drug release study of the chitosan-based nanoparticles. Heliyon. 2022;8(1):e08674. https://doi.org/10.1016/j.heliyon.2021.e08674
    PMid:35028457
21. Garg U, Chauhan S, Nagaich U, Jain N. Current advances in chitosan nanoparticles based drug delivery and targeting. Adv Pharm Bull. 2019;9(2):195-204. https://doi.org/10.15171/apb.2019.023
    PMid:31380245
22. Wimardhani YS, Suniarti DF, Freisleben HJ, Wanandi SI, Siregar NC, Ikeda MA. Chitosan exerts anticancer activity through induction of apoptosis and cell cycle arrest in oral cancer cells. J Oral Sci. 2014;56(2):119-26. https://doi.org/10.2334/josnusd.56.119
    PMid:24930748
23. Gupta N, Rajera R, Nagpal M, Arora S. Primaquine loaded chitosan nanoparticles for liver targeting. Pharm Nanotechnol. 2012;1:35-43.
24. Clogston JD, Patri AK. Zeta potential measurement. Methods Mol Biol. 2011;697:63-70. https://doi.org/10.1007/978-1-60327-198-1_6
    PMid:21116954
25. Selmani A, Kovačević D, Bohinc K. Nanoparticles: From synthesis to applications and beyond. Adv Colloid Interface Sci. 2022;303:102640. https://doi.org/10.1016/j.cis.2022.102640
    PMid:35358806
26. Liew KB, Janakiraman AK, Sundarapandian R, Khalid SH, Razzaq FA, Ming LC, *et al*. A review and revisit of nanoparticles for antimicrobial drug delivery. J Med Life. 2022;15(3):328-35. https://doi.org/10.25122/jml-2021-0097
    PMid:35449993
27. Sailaja AK, Amareshwar P, Chakravart. Chitosan Nanoparticles

as a Drug Delivery System. Res J Pharm Biol Chem Sci. 2010;1(3):474-84.

28. Baird K. Origins and implications of neglect of G6PD deficiency and primaquine toxicity in *Plasmodium vivax* malaria. Pathog Glob Health. 2015;109(3):93-106. https://doi.org/10.1179/2047773215Y.0000000016
PMid:25943156

29. Ashley EA, Recht J, White NJ. Primaquine: The risks and the benefits. Malar J. 2014;13:418. https://doi.org/10.1186/1475-2875-13-418
PMid:25363455

30. Mahmood I. Simple method for the estimation of absorption rate constant(ka)afteroraladministration.AmJTher.1998;5(6):377-82. https://doi.org/10.1097/00045391-199811000-00004
PMid:10099080

31. da Silva de Barros AO, Portilho FL, Dos Santos Matos AP, Ricci-Junior E, Alencar LM, Dos Santos CC, *et al*. Preliminary studies on drug delivery of polymeric primaquine microparticles using the liver high uptake effect based on size of particles to improve malaria treatment. Mater Sci Eng C Mater Biol Appl. 2021;128:112275. https://doi.org/10.1016/j.msec.2021.112275
PMid:34474834